

Learning-based Max-Min Fair Hybrid Precoding for mmWave Multicasting

Luis F. Abanto-Leon and Gek Hong (Allyson) Sim

Secure Mobile Networking (SEEMOO) Lab, Technische Universität Darmstadt, Germany

{labanto, asim}@seemoo.tu-darmstadt.de

Abstract—This paper investigates the joint design of hybrid transmit precoder and analog receive combiners for single-group multicasting in millimeter-wave systems. We propose LB-GDM, a low-complexity learning-based approach that leverages gradient descent with momentum and alternating optimization to design (i) the digital and analog constituents of a hybrid transmitter and (ii) the analog combiners of each receiver. In addition, we also extend our proposed approach to design fully-digital precoders. We show through numerical evaluation that, implementing LB-GDM in either hybrid or digital precoders attains superlative performance compared to competing designs based on semidefinite relaxation. Specifically, in terms of minimum signal-to-noise ratio, we report a remarkable improvement with gains of up to 105% and 101% for the fully-digital and hybrid precoders, respectively.

Index Terms—max-min fairness, hybrid precoding, multicast, millimeter-wave, learning, semidefinite relaxation.

I. INTRODUCTION

Wireless multicasting has a long-standing record for efficient utilization of spectrum resources to disseminate common information. Looking at the unprecedented growth in number and variety of multicast applications (e.g., high-definition video streaming, mobile video, content distribution in autonomous vehicular networks), multicast is outlined as a key player in emerging 5G millimeter-wave (mmWave) networks to sustain these demands [1]. With the recent advancements in antenna arrays architectures (e.g., digital-analog designs), particularly for mmWave systems, continuous investigation on beamforming techniques is crucial to ensure high performance. Indeed, a vital aspect to ensure high spectral efficiency lies in the optimal design of the beamformer or precoder. Nevertheless, the optimization problems derived from this context are at best non-convex quadratically constrained quadratic programs (QCQP), which have been proven NP-hard [2]. Therefore, many ongoing works are devoted to exploring alternative low-complexity schemes that yield near-optimality.

A. Related work

An initial work that addresses the NP-hardness of multicast optimization problems (e.g., quality-of-service (QoS) and max-min fairness (MMF)) in single-group scenarios is [2], where non-convex QCQPs are reformulated as semidefinite relaxation (SDR) programs. It is shown that SDR yields an approximate solution that, if feasible, is not necessarily optimum. To find feasible solutions, three types of Gaussian randomization are evaluated. In [3], an iterative algorithm based on second-order conic programming (SOCP) is proposed for the QoS problem

in single-group multicasting. The single-group MMF problem is studied in [4]. Furthermore, the QoS and MMF problems in multi-group multicast contexts are studied in [5]–[11].

The above-mentioned works consider beamforming using fully-digital precoders. In such an architecture, each antenna requires a dedicated baseband and a radio frequency (RF) chain, which is deemed impractical in many multi-antenna systems (e.g., mmWave) due to high design complexity, hardware cost, and power consumption. Consequently, industry and academia scrutinize antenna designs based on a digital-analog (hybrid) architectures which allow the use of a large number of antennas with a limited amount of RF chains [12]. While fully-digital precoders for physical layer multicasting has been widely researched, the design of hybrid precoders remains understudied. The existing literature on hybrid precoding includes investigations on the MMF (in [13], [14]) and QoS (in [15], [16]) problems for single-group and multi-group multicasting. However, the designs proposed therein are either (i) constrained due to simplified premises or (ii) unimplementable in the existing multi-antenna hardware, for the following reasons. In [14], the propounded solution requires a specially connected network of phase shifters for optimal operation. On the other hand, the proposed scheme in [16] is restricted to implementations with only four different phase shifts. In [15], the analog phase shifters are replaced by high-resolution lens arrays with adjustable power, thus circumventing the actual problem of phase shift selection. Finally, in [13], it is required to test several codewords in order to design the analog precoder, thus demanding additional memory storage that scales with the number of antennas.

Our objective is to provide a low-complexity scheme for already available off-the-shelf devices (e.g., TP-Link TALON AD7200), which reckon with a primitive network of phase shifters, limited memory storage, and moderate computational capabilities [17]. To address all these requirements, we propose a learning-based scheme that only requires matrix multiplications/additions with controllable complexity and performance that depend on customizable input parameters. Furthermore, in contrast to prior literature on multicasting, we include the design of analog multi-antenna combiners at the receivers.

B. Our contributions

We design the first learning-based hybrid precoder for single-group multicasting while considering analog multi-

antenna receivers. The details of our contributions are summarized as follows:

- We investigate the MMF problem subject to power constraints at the transmitter and receivers. Precisely, our solution can handle an arbitrary number of constant-modulus phase shifts for the analog precoder in contrast to the existing designs that only consider a limited number of phase shifts. Moreover, the idea is extended for designing the analog combiners at the receivers.
- Our proposed learning-based scheme has lower complexity than SDR-based approaches. While SDR-based solutions require expensive vector-lifting that expands the variables into higher dimensional spaces, our proposed scheme, namely LB-GDM, only uses matrix multiplications/additions and a number of low-dimensional matrix inversions. Furthermore, the exploration and exploitation phases of our algorithm promote the search for optimal solutions while preventing getting trapped in local optima. Specifically, LB-GDM leverages gradient descent with momentum and alternating optimization.
- We consider analog multi-antenna receivers. We show that, by endowing the receivers with only two antennas, the minimum SNR improves by 75.7% compared to omnidirectional receiving patterns (i.e., single antenna case).
- Since the SDR method in [2] is only applicable to fully-digital implementations, we propose a novel scheme called SDR-C, capable of handling the constant-modulus constraints of the hybrid precoder and analog receivers. Inspired by [18], SDR-C exploits SDR and Cholesky matrix factorization. A similar technique was used by [19] to solve the QoS problem for multi-group multicasting. We extend the idea in [19] to the MMF problem.
- We perform extensive simulations to evaluate the performance of LB-GDM and SDR-C in terms of minimum SNR and spectral efficiency. We provide valuable insights on the fully-digital and hybrid precoders design under various system parameters (i.e., the number of transmit and receive antennas, the number of RF chains, and the number of iterations). We show that LB-GDM substantially outperforms state-of-the-art SDR-based solutions such as SDR-C, achieving up to 105.6% and 101.4% gains in digital and hybrid precoders, respectively.

II. SYSTEM MODEL

We consider a mmWave system where a next generation Node B (gNodeB) serves a set of K multicast users denoted by $\mathcal{K} = \{1, 2, \dots, K\}$. The gNodeB is equipped with N_{tx} transmit antennas and $N_{\text{tx}}^{\text{RF}}$ radio frequency (RF) chains, where $N_{\text{tx}}^{\text{RF}} \leq N_{\text{tx}}$. The downlink signal is represented by $\mathbf{x} = \mathbf{F}\mathbf{m}s$, where $\mathbf{F} \in \mathbb{C}^{N_{\text{tx}} \times N_{\text{tx}}^{\text{RF}}}$ and $\mathbf{m} \in \mathbb{C}^{N_{\text{tx}}^{\text{RF}} \times 1}$ are the analog and digital components of the hybrid precoder. The data symbol s has unit power in average, i.e., $\mathbb{E}\{ss^*\} = 1$. Every element of the analog precoder is a phase rotation with constant modulus, i.e., $[\mathbf{F}]_{q,r} \in \mathcal{F} = \left\{ \sqrt{\delta_{\text{tx}}}, \dots, \sqrt{\delta_{\text{tx}}} e^{j \frac{2\pi(L_{\text{tx}}-1)}{L_{\text{tx}}}} \right\}$, where $q \in \mathcal{Q} = \{1, \dots, N_{\text{tx}}\}$, $r \in \mathcal{R} = \{1, \dots, N_{\text{tx}}^{\text{RF}}\}$ and L_{tx} is the number of allowed phase

rotation values. Each user is endowed with $N_{\text{rx}} \ll N_{\text{tx}}$ antennas and an analog combiner $\mathbf{w}_k \in \mathbb{C}^{N_{\text{rx}} \times 1}$ with $N_{\text{rx}}^{\text{RF}} = 1$, such that $[\mathbf{w}_k] \in \mathcal{W} = \left\{ \sqrt{\delta_{\text{rx}}}, \dots, \sqrt{\delta_{\text{rx}}} e^{j \frac{2\pi(L_{\text{rx}}-1)}{L_{\text{rx}}}} \right\}$, $l \in \mathcal{L} = \{1, \dots, N_{\text{rx}}\}$ and L_{rx} is the number of allowed phase rotation possibilities at the receivers. Under the assumption of narrowband flat-fading, the signal received by the k -th user is

$$y_k = \underbrace{\mathbf{w}_k^H \mathbf{H}_k \mathbf{F} \mathbf{m} s}_{\text{multicast signal}} + \underbrace{\mathbf{w}_k^H \mathbf{n}_k}_{\text{noise}}, \quad (1)$$

where $\mathbf{H}_k \in \mathbb{C}^{N_{\text{rx}} \times N_{\text{tx}}}$ denotes the channel between the k -th user and the gNodeB, whereas $\mathbf{n}_k \sim \mathcal{CN}(\mathbf{0}, \sigma^2 \mathbf{I})$ denotes additive white Gaussian noise. The SNR at user k is given by

$$\gamma_k = \frac{|\mathbf{w}_k^H \mathbf{H}_k \mathbf{F} \mathbf{m}|^2}{\sigma^2 \|\mathbf{w}_k\|_2^2}. \quad (2)$$

III. PROBLEM FORMULATION

The objective is to design a hybrid precoder that maximizes the minimum SNR among all K users, subject to power constraints at the transmitter and receiver. We define

$$\mathcal{P}_0^{\text{hyb}} : \max_{\mathbf{F}, \mathbf{m}, \{\mathbf{w}_k\}_{k=1}^K} \min_{k \in \mathcal{K}} \frac{|\mathbf{w}_k^H \mathbf{H}_k \mathbf{F} \mathbf{m}|^2}{\sigma^2 \|\mathbf{w}_k\|_2^2} \quad (3a)$$

$$\text{s.t.} \quad \|\mathbf{F} \mathbf{m}\|_2^2 = P_{\text{tx}}^{\text{max}}, \quad (3b)$$

$$\|\mathbf{F}\|_{\text{F}}^2 = 1, \quad (3c)$$

$$[\mathbf{F}]_{q,r} \in \mathcal{F}, q \in \mathcal{Q}, r \in \mathcal{R}, \quad (3d)$$

$$\|\mathbf{w}_k\|_2^2 = P_{\text{rx}}^{\text{max}}, k \in \mathcal{K}, \quad (3e)$$

$$[\mathbf{w}_k]_l \in \mathcal{W}, l \in \mathcal{L}, \forall k \in \mathcal{K}, \quad (3f)$$

where (3b) restricts the transmit power of the hybrid precoder, (3c) imposes a power normalization on the phase rotations, (3d) enforces every phase rotation of the analog precoder to be in \mathcal{F} , (3e) restrains the receive power whereas (3f) constrains the phase rotations of the combiners to \mathcal{W} . The constraints (3d) and (3f) denote non-convex feasible sets due to their combinatorial nature. Also, due to parameter coupling, (3b) is non-convex. The objective function (3a) is defined as the ratio of two quadratic expressions, where the numerator exhibits coupling of three parameters. Thus, $\mathcal{P}_0^{\text{hyb}}$ is a non-convex problem. Note that (3c) and (3e) can be circumvented as they are only employed to calculate $\delta_{\text{tx}} = 1/N_{\text{tx}}^{\text{RF}} N_{\text{tx}}$ and $\delta_{\text{rx}} = P_{\text{rx}}^{\text{max}}/N_{\text{rx}}$.

Remark: When $N_{\text{rx}} = 1$, $\{\mathbf{w}_k\}_{k=1}^K = 1$, and $\mathbf{F} = \mathbf{I}$, $\mathcal{P}_0^{\text{hyb}}$ collapses to the problem investigated in [2], which is known to be NP-hard. Since (3) has additional non-convex constraints, $\mathcal{P}_0^{\text{hyb}}$ is thus NP-hard as well. Additionally, when $N_{\text{rx}} = 1$ and $\{\mathbf{w}_k\}_{k=1}^K = 1$, $\mathcal{P}_0^{\text{hyb}}$ is equivalent to the problem studied in [13].

IV. PROPOSED SCHEME

In order to solve (3), we adopt an alternating optimization approach that allows us to decouple the unknown parameters \mathbf{F} , \mathbf{m} , and $\{\mathbf{w}_k\}_{k=1}^K$. Thus, $\mathcal{P}_0^{\text{hyb}}$ in (3) is decomposed into three sub-problems $\mathcal{P}_1^{\text{hyb}}$, $\mathcal{P}_2^{\text{hyb}}$, and $\mathcal{P}_3^{\text{hyb}}$ defined in (4), (9), and (11), respectively. Moreover, for each of the sub-problems we propose a learning-based algorithm that leverages gradient

Algorithm 1: Optimization of the analog precoder

Input: The precoders $\mathbf{F}^{(t-1)}$, $\mathbf{m}^{(t-1)}$ and receive combiners $\{\mathbf{w}_k^{(t-1)}\}_{k=1}^K$
Output: The analog precoder $\mathbf{F}^{(t)}$
Execute:
1: Calculate the weights $c_k^{(t)}$, $\forall k \in \mathcal{K}$.
2: Compute $\nabla J^F = \sum_{k=1}^K c_k^{(t)} \nabla_{\mathbf{F}} J_k^F / \|\nabla_{\mathbf{F}} J_k^F\|_{\mathbf{F}}$.
3: Compute the normalized gradient $\nabla \tilde{J}_F^{(t)} = \nabla J^F / \|\nabla J^F\|_{\mathbf{F}}$.
4: Compute $\mathbf{F}^{(t)} = \mathbf{F}^{(t-1)} + \rho_F \mathbf{F}_{\text{best}}^{(t-1)} + \alpha_F \nabla \tilde{J}_F^{(t)}$.
5: Project $[\mathbf{F}^{(t)}]_{q,r} \leftarrow \Pi_{\mathcal{F}} [\mathbf{F}^{(t)}]_{q,r}$ onto \mathcal{F} to satisfy (8b).

descent with momentum, i.e., LB-GDM. Conversely to [20], where the momentum term affects the most recent gradient, in our case the momentum is associated with the fittest known solution (at each iteration). Furthermore, we include two parameters, N_{xpr} and N_{xpt} , that control exploration and exploitation of the learning process, respectively.

A. Optimization of the analog precoder \mathbf{F}

Assuming that \mathbf{m} and $\{\mathbf{w}_k\}_{k=1}^K$ are known, we optimize \mathbf{F} ,

$$\mathcal{P}_1^{\text{hyb}} : \max_{\mathbf{F}} \min_{k \in \mathcal{K}} \frac{|\mathbf{w}_k^H \mathbf{H}_k \mathbf{F} \mathbf{m}|^2}{\sigma^2 P_{\text{tx}}^{\max}} \quad (4a)$$

$$\text{s.t.} \quad \|\mathbf{F} \mathbf{m}\|_2^2 = P_{\text{tx}}^{\max}, \quad (4b)$$

$$[\mathbf{F}]_{q,r} \in \mathcal{F}, q \in \mathcal{Q}, r \in \mathcal{R}. \quad (4c)$$

In order to reduce the number of constraints, we incorporate (4b) into the objective function (4a). Specifically, we replace $\frac{|\mathbf{w}_k^H \mathbf{H}_k \mathbf{F} \mathbf{m}|^2}{\sigma^2 P_{\text{tx}}^{\max}} = \psi \frac{|\mathbf{w}_k^H \mathbf{H}_k \mathbf{F} \mathbf{m}|^2}{\|\mathbf{F} \mathbf{m}\|_2^2}$, where $\psi = \frac{P_{\text{tx}}^{\max}}{\sigma^2 P_{\text{tx}}^{\max}}$. Notice that ψ can be disregarded as it is constant for all the users. Thus,

$$\bar{\mathcal{P}}_1^{\text{hyb}} : \max_{\mathbf{F}} \min_{k \in \mathcal{K}} \frac{\mathbf{m}^H \mathbf{F}^H \mathbf{H}_k^H \mathbf{w}_k \mathbf{w}_k^H \mathbf{H}_k \mathbf{F} \mathbf{m}}{\mathbf{m}^H \mathbf{F}^H \mathbf{F} \mathbf{m}} \quad (5a)$$

$$\text{s.t.} \quad [\mathbf{F}]_{q,r} \in \mathcal{F}, q \in \mathcal{Q}, r \in \mathcal{R}. \quad (5b)$$

Instead of approaching (5), we propose to solve the surrogate problem (6), which consists of a weighted sum of all $\tau_k^F = \frac{\mathbf{m}^H \mathbf{F}^H \mathbf{H}_k^H \mathbf{w}_k \mathbf{w}_k^H \mathbf{H}_k \mathbf{F} \mathbf{m}}{\mathbf{m}^H \mathbf{F}^H \mathbf{F} \mathbf{m}}$, as shown in (6)

$$\hat{\mathcal{P}}_1^{\text{hyb}} : \max_{\mathbf{F}} \sum_{k=1}^K c_k \frac{\mathbf{m}^H \mathbf{F}^H \mathbf{H}_k^H \mathbf{w}_k \mathbf{w}_k^H \mathbf{H}_k \mathbf{F} \mathbf{m}}{\mathbf{m}^H \mathbf{F}^H \mathbf{F} \mathbf{m}} \quad (6a)$$

$$\text{s.t.} \quad [\mathbf{F}]_{q,r} \in \mathcal{F}, q \in \mathcal{Q}, r \in \mathcal{R}, \quad (6b)$$

where $c_k \geq 0$ denotes the k -th weighting factor. On the other hand, note that τ_k^F is upper-bounded by

$$\begin{aligned} \tau_k^F &\leq \lambda_{\max} \left((\mathbf{F}^H \mathbf{F})^{-1} \mathbf{F}^H \mathbf{H}_k^H \mathbf{w}_k \mathbf{w}_k^H \mathbf{H}_k \mathbf{F} \right) \\ &= \underbrace{\mathbf{w}_k^H \mathbf{H}_k \mathbf{F} (\mathbf{F}^H \mathbf{F})^{-1} \mathbf{F}^H \mathbf{H}_k^H \mathbf{w}_k}_{J_k^F}, \end{aligned} \quad (7)$$

where $\lambda_{\max}(\cdot)$ extracts the maximum eigenvalue of matrix $(\mathbf{F}^H \mathbf{F})^{-1} \mathbf{F}^H \mathbf{H}_k^H \mathbf{w}_k \mathbf{w}_k^H \mathbf{H}_k \mathbf{F}$. Upon replacing τ_k^F in (6) by its upper bound J_k^F , the problem collapses to

$$\tilde{\mathcal{P}}_1^{\text{hyb}} : \max_{\mathbf{F}} \sum_{k=1}^K c_k \mathbf{w}_k^H \mathbf{H}_k \mathbf{F} (\mathbf{F}^H \mathbf{F})^{-1} \mathbf{F}^H \mathbf{H}_k^H \mathbf{w}_k, \quad (8a)$$

$$\text{s.t.} \quad [\mathbf{F}]_{q,r} \in \mathcal{F}, q \in \mathcal{Q}, r \in \mathcal{R}. \quad (8b)$$

Since (8a) is an upper bound for (6a), an optimal solution to (8), in general, may not be optimal to (6). Notice that the performance of the system in (8) will be determined by the

Algorithm 2: Optimization of the digital precoder

Input: The precoders $\mathbf{F}^{(t)}$, $\mathbf{m}^{(t-1)}$ and receive combiners $\{\mathbf{w}_k^{(t-1)}\}_{k=1}^K$
Output: The digital precoder $\mathbf{m}^{(t)}$
Execute:
1: Calculate the weights $d_k^{(t)}$, $\forall k \in \mathcal{K}$.
2: Compute $\nabla J^M = \sum_{k=1}^K d_k^{(t)} \nabla_{\mathbf{m}} J_k^M / \|\nabla_{\mathbf{m}} J_k^M\|_2$.
3: Compute the normalized gradient $\nabla \tilde{J}_M^{(t)} = \nabla J^M / \|\nabla J^M\|_2$.
4: Compute $\mathbf{m}^{(t)} = \mathbf{m}^{(t-1)} + \rho_M \mathbf{m}_{\text{best}}^{(t-1)} + \alpha_M \nabla \tilde{J}_M^{(t)}$.
5: Normalize $\mathbf{m}^{(t)} \leftarrow \sqrt{P_{\text{tx}}^{\max}} \mathbf{m}^{(t)} / \|\mathbf{F} \mathbf{m}^{(t)}\|_2$.

minimum J_k^F , which can be regarded as a utility function of the k -th user. In order to solve (8), we first compute the gradient of $\sum_{k=1}^K c_k J_k^F$ to update \mathbf{F} . Then, we scale the modulus of each $[\mathbf{F}]_{q,r}$ and approximate its phase by the closest available option in \mathcal{F} in order to comply with (8b), as detailed in Algorithm 1. The gradient of J_k^F with respect to \mathbf{F} is $\nabla_{\mathbf{F}} J_k^F = (\mathbf{I} - \mathbf{F} \mathbf{F}^\dagger)^T (\mathbf{F}^\dagger \mathbf{H}_k^H \mathbf{w}_k \mathbf{w}_k^H \mathbf{H}_k)^T$, where $\mathbf{F}^\dagger = (\mathbf{F}^H \mathbf{F})^{-1} \mathbf{F}^H$ (see Appendix for derivation). In *Step 1*, the weights are computed according to $c_k^{(t)} = \left(1 + \xi \left(\gamma_{\max}^{(t-1)} - \gamma_k^{(t-1)}\right) / \gamma_{\max}^{(t-1)}\right)^2$ for each iteration t , where $\gamma_k^{(t)}$ is the SNR attained by user k , $\gamma_{\max}^{(t)} = \max_{k \in \mathcal{K}} \gamma_k^{(t)}$ and $\xi > 0$. In *Step 2*, the weighted sum of the unit-power gradients $\nabla_{\mathbf{F}} J_k^F / \|\nabla_{\mathbf{F}} J_k^F\|_{\mathbf{F}}$ is computed. In *Step 3*, the unit-power aggregate gradient $\nabla \tilde{J}_F^{(t)}$ is obtained. In *Step 4*, the current $\mathbf{F}^{(t-1)}$ is updated using $\nabla \tilde{J}_F^{(t)}$. Also, $\mathbf{F}_{\text{best}}^{(t)}$ represents the best known solution until iteration t , whereas ρ_F and α_F are the momentum and learning factors associated to \mathbf{F} , respectively. Finally, *Step 5* enforces (8b). The weights are bounded to $1 \leq c_k^{(t)} \leq (1 + \xi)^2$ and increase inversely proportional to the attained SNR $\gamma_k^{(t)}$. Thus, the gradient of the user with minimum SNR is weighted with the largest $c_k^{(t)}$, whereas the gradient of the user with maximum SNR is assigned the smallest $c_k^{(t)} = 1$.

Remark: To motivate the connection between (5) and (6), we assume that (6) can be solved iteratively, and in each iteration we are capable of predicting $k^* = \arg \min_{k \in \mathcal{K}} \tau_k^F$. Thus, if we assigned binary values $c_{k^*} = 1$ and $c_{k \neq k^*} = 0$ at each iteration instance, we would indirectly be solving a problem closely related to (5), where the minimum SNR is maximized. However, due to the intractability of predicting such k^* , we propose to simultaneously maximize a subset of the smallest SNRs by considering non-binary positive weights $c_k^{(t)}$ that can be adapted based on the SNR values (obtained after each iteration), thus controlling the priorities of τ_k^F or J_k^F . This proposed approach also facilitates to keep track of several gradients simultaneously, preventing the search from getting trapped in local optima.

B. Optimization of the digital precoder \mathbf{m}

When \mathbf{F} and $\{\mathbf{w}_k\}_{k=1}^K$ are known, the problem collapses to

$$\mathcal{P}_2^{\text{hyb}} : \max_{\mathbf{m}} \min_{k \in \mathcal{K}} \left| \mathbf{w}_k^H \mathbf{H}_k \mathbf{F} \mathbf{m} \right|^2 \quad (9a)$$

$$\text{s.t.} \quad \|\mathbf{F} \mathbf{m}\|_2^2 = P_{\text{tx}}^{\max}. \quad (9b)$$

Algorithm 3: Optimization of the k -th combiner

Input: The precoders $\mathbf{F}^{(t)}$, $\mathbf{m}^{(t)}$ and the receive combiner $\mathbf{w}_k^{(t-1)}$

Output: The receive combiner $\mathbf{w}_k^{(t)}$

Execute:

- 1: Compute $\nabla_{\mathbf{w}_k} J_k^W$.
 - 2: Compute $\nabla_{\mathbf{w}_k} \tilde{J}_W^{(t)} = \nabla_{\mathbf{w}_k} J_k^W / \|\nabla_{\mathbf{w}_k} J_k^W\|_2$.
 - 3: Compute $\mathbf{w}_k^{(t)} = \mathbf{w}_k^{(t-1)} + \rho_W \mathbf{w}_{\text{best},k}^{(t-1)} + \alpha_W \nabla_{\mathbf{w}_k} \tilde{J}_W^{(t)}$.
 - 4: Project $[\mathbf{w}_k^{(t)}]_l \leftarrow \Pi_{\mathcal{W}} [\mathbf{w}_k^{(t)}]_l$ onto \mathcal{W} , $\forall l \in \mathcal{L}$ to satisfy (12b).
-

Similarly as in (5) and (6), we recast (9) as

$$\tilde{\mathcal{P}}_2^{\text{hyb}} : \max_{\mathbf{m}} \sum_{k=1}^K d_k \left| \mathbf{w}_k^H \mathbf{H}_k \mathbf{F} \mathbf{m} \right|^2 \quad (10a)$$

$$\text{s.t.} \quad \|\mathbf{F} \mathbf{m}\|_2^2 = P_{\text{tx}}^{\text{max}}, \quad (10b)$$

where d_k is the weight corresponding to $J_k^M = |\mathbf{w}_k^H \mathbf{H}_k \mathbf{F} \mathbf{m}|^2$. Compared to $\tilde{\mathcal{P}}_1^{\text{hyb}}$, where an upper bound J_k^M for τ_k^F was derived, finding such a bound by means of the same procedure is not feasible in this case, as it involves computing the inverse of a rank-1 matrix $M = \mathbf{m}^* \mathbf{m}^T$. Thus, we assume $J_k^M = \tau_k^M$. $\tilde{\mathcal{P}}_2^{\text{hyb}}$ is iteratively solved employing Algorithm 2, where a similar procedure as in Algorithm 1 is used to compute \mathbf{m} . Moreover, we assume that $d_k^{(t)}$ are computed in the same fashion as $c_k^{(t)}$. The gradient of J_k^M with respect to \mathbf{m} is $\nabla_{\mathbf{m}} J_k^M = \mathbf{m}^H \mathbf{F}^H \mathbf{H}_k^H \mathbf{w}_k \mathbf{w}_k^H \mathbf{H}_k \mathbf{F}$. The main difference between Algorithm 1 and Algorithm 2 is *Step 5*, which restricts the transmit power to $P_{\text{tx}}^{\text{max}}$.

C. Optimization of the combiners \mathbf{w}_k

Assuming that \mathbf{F} and \mathbf{m} are given, we optimize $\{\mathbf{w}_k\}_{k=1}^K$

$$\mathcal{P}_3^{\text{hyb}} : \max_{\{\mathbf{w}_k\}_{k=1}^K} \min_{k \in \mathcal{K}} \frac{|\mathbf{w}_k^H \mathbf{H}_k \mathbf{F} \mathbf{m}|^2}{\sigma^2 \|\mathbf{w}_k\|_2^2} \quad (11a)$$

$$\text{s.t.} \quad [\mathbf{w}_k]_l \in \mathcal{W}, l \in \mathcal{L}, \forall k \in \mathcal{K}. \quad (11b)$$

Note that (11) can be decomposed into K parallel and independent sub-problems, whereby users will adapt their corresponding \mathbf{w}_k in order to maximize their own SNR. Also, since $\|\mathbf{w}_k\|_2^2$ is a scalar, each sub-problem reduces to

$$\tilde{\mathcal{P}}_{3,k}^{\text{hyb}} : \max_{\mathbf{w}_k} \left| \mathbf{w}_k^H \mathbf{H}_k \mathbf{F} \mathbf{m} \right|^2 \quad (12a)$$

$$\text{s.t.} \quad [\mathbf{w}_k]_l \in \mathcal{W}, l \in \mathcal{L}, \quad (12b)$$

$\forall k \in \mathcal{K}$. As in $\tilde{\mathcal{P}}_2^{\text{hyb}}$, we assume $J_k^W = \tau_k^W = |\mathbf{w}_k^H \mathbf{H}_k \mathbf{F} \mathbf{m}|^2$. Moreover, each sub-problem in (12) is similar to (8) except that each user optimizes their own utility function J_k^W . We employ Algorithm 3 to find $\{\mathbf{w}_k\}_{k=1}^K$, where $\nabla_{\mathbf{w}_k} J_k^W = \mathbf{w}_k^H \mathbf{H}_k \mathbf{F} \mathbf{m} \mathbf{m}^H \mathbf{F}^H \mathbf{H}_k^H$.

For completeness, LB-GDM is summarized in Algorithm 4. The exploration phase is based on randomization of \mathbf{F} , \mathbf{m} and $\{\mathbf{w}_k\}_{k=1}^K$ (line 17). The exploitation phase harnesses $\mathbf{F}_{\text{best}}^{(t)}$, $\mathbf{m}_{\text{best}}^{(t)}$, and $\{\mathbf{w}_{\text{best},k}^{(t)}\}_{k=1}^K$ as the momentum terms, which preserve the fittest known solutions until iteration t and are updated once per exploration instance (line 16). On the other hand, \mathbf{F}_{opt} , \mathbf{m}_{opt} , and $\{\mathbf{w}_{\text{opt},k}^{(t)}\}_{k=1}^K$ retain the fittest solutions after each exploitation instance (line 10). These parameters are updated more frequently since they execute a finer scanning of the search space. Further, to refine the potential solutions in this phase, the learning factors α_F , α_M and α_W are progressively

Algorithm 4: Proposed LB-GDM scheme

Initialize:

- 1: Assign $[\mathbf{F}^{(0)}]_{q,r} \leftarrow \delta$, $q = \{1, \dots, N_{\text{tx}}\}$, $r \leftarrow \text{mod}(q, N_{\text{tx}}^{\text{RF}}) + 1$,
 $\mathbf{m}^{(0)} \leftarrow [1 \mathbf{0}_{1 \times (N_{\text{tx}}^{\text{RF}} - 1)}]^T$, $\mathbf{w}_k^{(0)} \leftarrow [1 \mathbf{0}_{1 \times (N_{\text{rx}} - 1)}]^T$, $\forall k \in \mathcal{K}$.
- 2: Assign $\mathbf{F}_{\text{best}} \leftarrow \mathbf{0}$, $\mathbf{m}_{\text{best}} \leftarrow \mathbf{0}$ and $\{\mathbf{w}_{\text{best},k}\} \leftarrow \mathbf{0}$.
- 3: Assign $\alpha_F \leftarrow \alpha_{F_0}$, $\alpha_M \leftarrow \alpha_{M_0}$, $\alpha_W \leftarrow \alpha_{W_0}$.
- 4: Assign $t \leftarrow 0$, $\gamma_T \leftarrow 0$.

Execute:

- 5: **for** $i_{\text{xpr}} = 1, \dots, N_{\text{xpr}}$ **do** (exploration phase)
 - 6: **for** $i_{\text{xpt}} = 1, \dots, N_{\text{xpt}}$ **do** (exploitation phase)
 - 7: Compute $\mathbf{F}^{(t)}$, $\mathbf{m}^{(t)}$, $\{\mathbf{w}_k^{(t)}\}_{k=1}^K$ via Algorithms 1, 2, 3.
 - 8: Find the minimum SNR, γ_{min} , among all users.
 - 9: **if** $\gamma_{\text{min}} \geq \gamma_T$
 - 10: Assign $\mathbf{F}_{\text{opt}} \leftarrow \mathbf{F}^{(t)}$, $\mathbf{m}_{\text{opt}} \leftarrow \mathbf{m}^{(t)}$, $\{\mathbf{w}_{\text{opt},k}\}_{k=1}^K \leftarrow \{\mathbf{w}_k^{(t)}\}_{k=1}^K$.
 - 11: Assign $\gamma_T \leftarrow \gamma_{\text{min}}$.
 - 12: **end if**
 - 13: Update $\alpha_F \leftarrow 0.98 \alpha_F$, $\alpha_M \leftarrow 0.98 \alpha_M$, $\alpha_W \leftarrow 0.98 \alpha_W$.
 - 14: Increment $t \leftarrow t + 1$.
 - 15: **end for**
 - 16: Assign $\mathbf{F}_{\text{best}}^{(t)} \leftarrow \mathbf{F}_{\text{opt}}$, $\mathbf{m}_{\text{best}}^{(t)} \leftarrow \mathbf{m}_{\text{opt}}$, $\{\mathbf{w}_{\text{best},k}^{(t)}\}_{k=1}^K \leftarrow \{\mathbf{w}_{\text{opt},k}^{(t)}\}_{k=1}^K$.
 - 17: Randomize $\mathbf{F}^{(t)}$, $\mathbf{m}^{(t)}$ and $\{\mathbf{w}_k^{(t)}\}_{k=1}^K$ enforcing (3b) - (3f).
 - 18: Assign $\alpha_F \leftarrow \alpha_{F_0}$, $\alpha_M \leftarrow \alpha_{M_0}$, $\alpha_W \leftarrow \alpha_{W_0}$.
 - 19: **end for**
-

decreased as the exploration phase advances (line 13). However, these learning factors are reset to their original values when a new exploration instance begins (line 18). A proper balance between exploration and exploitation allows LB-GDM to produce more suitable precoders than SDR.

V. SIMULATION RESULTS

We consider the geometric channel model with $N_p = 5$ propagation paths between the transmitter and each user. Also, $P_{\text{tx}}^{\text{max}} = 1$ (30 dBm), $P_{\text{rx}}^{\text{max}} = 0.01$ (10 dBm), $\sigma^2 = 1$ (30 dBm), while \mathcal{F} and \mathcal{W} consist of $L_{\text{tx}} = 8$ and $L_{\text{rx}} = 4$ different phase shifts, respectively. In the following scenarios, we compare the performance of LB-GDM and SDR-C for fully-digital and hybrid precoders in terms of the minimum SNR (among all users) and the spectral efficiency (SE), computed as the sum-capacity of the whole system. We evaluate several configurations of N_{tx} , $N_{\text{tx}}^{\text{RF}}$, N_{rx} , N_{xpr} , N_{xpt} , and K . For LB-GDM, we set $\rho_F = \rho_M = \rho_W = 0.9$, $\alpha_{F_0} = 1$, $\alpha_{M_0} = 1$, $\alpha_{W_0} = 1$ and vary N_{xpr} , N_{xpt} to control the fitness of the solutions. In the case of SDR-C, we control the number of randomizations N_{rand} . Furthermore, the numerical results show the average over 100 channel realizations.

A. Impact of exploration (N_{xpr}) and exploitation (N_{xpt})

In this scenario we evaluate the performance of LB-GDM for different values of N_{xpr} and N_{xpt} , under a particular channel realization. We consider $K = 30$, $N_{\text{tx}} = 15$, $N_{\text{rx}} = 2$, when N_{xpr} and N_{xpt} are varied in the range $[1, 100]$. For the fully-digital and hybrid precoders, we assume $N_{\text{tx}}^{\text{RF}} = N_{\text{tx}} = 15$ and $N_{\text{tx}}^{\text{RF}} = 6$, respectively. We observe in Fig. 1 that the minimum SNR improves for increasing values of N_{xpr} and N_{xpt} in both precoders. Further, N_{xpr} is more relevant than N_{xpt} in improving this metric for this particular realization. Nevertheless, both of these phases are important. Exploration is the capability of effectively sampling/scanning the search space to find potentially fitter solutions, whereas exploitation

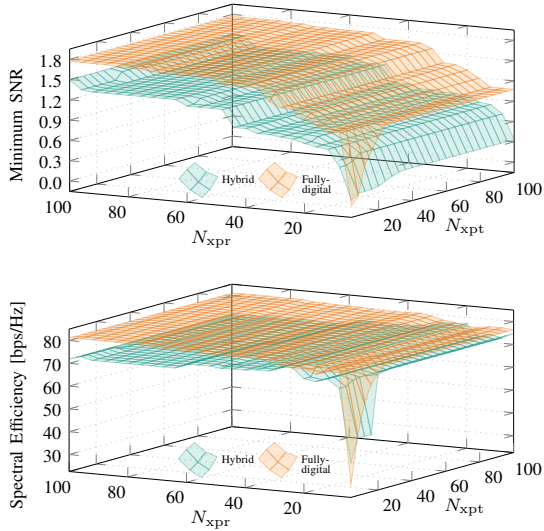


Figure 1: Impact of exploration (N_{xpr}) and exploitation (N_{xpt}) phases on the system performance.

capitalizes on already known solutions to further refine them. By doing so, our proposed LB-GDM avoids getting trapped in local optima. As expected, the fully-digital precoder outperforms its hybrid counterpart due to a larger number of RF chains and less stringent constraints (constant-modulus phase shifts). The former attains a minimum SNR of 1.77 whereas the latter achieves 1.49. Besides, the hybrid precoder attains 11.5% lower SE than that of the fully-digital precoder.

Remark: While the minimum SNR monotonically increases for both precoders, the SE performance does not exhibit the same behavior. This is because the optimization criterion of LB-GDM is to enhance the minimum SNR (MMF), without considering the spectral efficiency. Nevertheless, the general trend shows that higher N_{xpr} and N_{xpt} yield SE improvement.

B. Impact of the number of antennas N_{tx} and N_{rx}

In this scenario, we evaluate the performance of hybrid and fully-digital precoders based on LB-GDM for a different number of transmit and receive antennas. We consider $K = 50$, $N_{tx} = \{8, 12, 16\}$, and $N_{rx} = \{1, 2, 3, 4, 5\}$. For the hybrid precoder, we assume $N_{tx}^{RF} = 2$. Fig. 2 depicts the improvement of the minimum SNR when increasing N_{tx} and N_{rx} , for both types of precoders. Since the transmit and receive power are limited, endowing users with multiple antennas is beneficial to improve the SNR. In particular, in the fully-digital case, when $N_{tx} = 8$, the minimum SNR improves from 0.37 to 0.65 when the number of receive antenna increases from $N_{rx} = 1$ to $N_{rx} = 2$, which essentially indicates a 75.7% gain. Similarly, the gain for the hybrid precoder is 100%. We also observe a considerable improvement of the minimum SNR as N_{tx} increases from 8 to 16, in which we attain a gain of up to 72.9% and 58.6% for fully-digital and hybrid precoders, respectively. Further, the SE also achieves 25.5% and 32.9% gain, for the fully-digital and hybrid precoders, respectively (when $N_{tx} = 8$, for $N_{rx} = 1$ and $N_{rx} = 2$). In general, the hybrid precoder attains a SE at worst 11.8% lower than its fully-digital counterpart (for

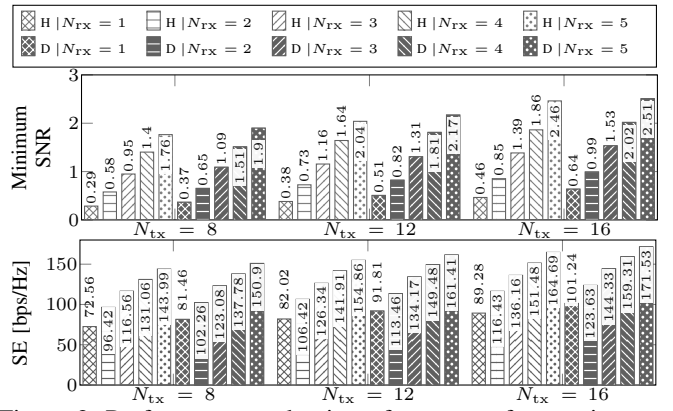
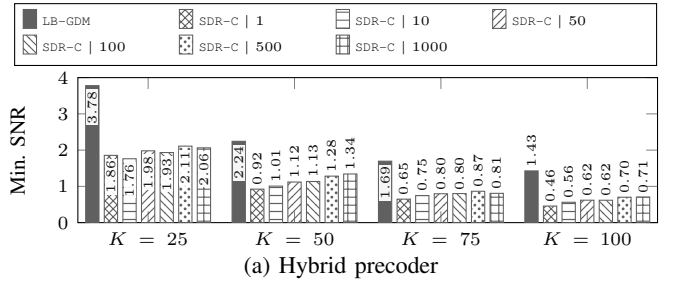
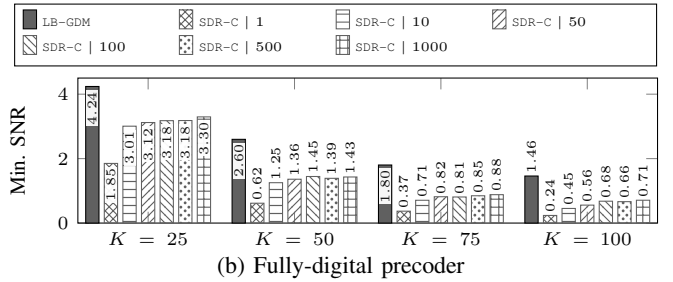


Figure 2: Performance evaluation of LB-GDM for varying N_{tx} and N_{rx} in fully-digital (D) and hybrid (H) precoders.



(a) Hybrid precoder



(b) Fully-digital precoder

Figure 3: Performance comparison between LB-GDM and SDR-C in terms of the minimum SNR.

all the cases). We also observe that with only $N_{rx}^{RF} = 2$, the hybrid transmit precoder is at worst 25.5% below the optimality attained by the fully-digital in terms of the minimum SNR.

Remark: This scenario sheds lights on the relevance of reckoning with multiple antennas at the receivers when constrained by power at both ends. Specifically, we obtain improvements up to 72.9% and 58.6% by increasing the number of receive antennas from $N_{rx} = 1$ to $N_{rx} = 2$. On the other hand, in this case where $N_{tx}^{RF} = 2$, the complexity of LB-GDM is even more affordable as $\mathbf{F}^\dagger = (\mathbf{F}^H \mathbf{F})^{-1} \mathbf{F}^H$ requires no actual inversion of $\mathbf{F}^H \mathbf{F}$, since a 2×2 matrix can be inverted directly.

C. Performance comparison with an SDR-based scheme

We compare the performance of LB-GDM and SDR-C, when implemented in fully-digital and hybrid precoders. We consider $N_{tx} = 20$, $N_{rx} = 3$, with a wide range of users $K = \{25, 50, 75, 100\}$. For the hybrid precoder $N_{tx}^{RF} = 6$, whereas for the fully-digital counterpart $N_{tx}^{RF} = N_{tx}$. For LB-GDM, we assume that $N_{xpt} = N_{xpr} = 120$. For SDR-C, the number of randomizations are $N_{rand} = \{1, 10, 50, 100, 500, 1000\}$. To ensure a fair comparison, we refine the solutions of SDR-C by

optimizing sequentially \mathbf{F} , \mathbf{m} , and $\{\mathbf{w}_k\}_{k=1}^K$ over $N_{\text{iter}}^{\text{SDR}} = 3$ iterations. In each iteration, N_{rand} randomizations are evaluated. Fig. 3 depicts a notable improvement of LB-GDM over SDR-C in both fully-digital (see Fig. 3b) and hybrid (see Fig. 3a) implementations, for all K . Specifically, the SDR-C results are shown in the format $\langle \text{SDR-C} \mid N_{\text{rand}} \rangle$. We observe a more prominent improvement for larger K . For instance, in the case of the fully-digital precoder, when $K = 50$, the minimum SNR obtained by LB-GDM is 79.3% higher than that of SDR-C although a wide range of N_{rand} were tested. The gain is even higher (i.e. 105.6%) for $K = 100$. We observe a similar trend for LB-GDM-based hybrid precoder, with gains of up to 101.4%.

VI. DISCUSSION

SDR-C: This scheme is based on the approach in [19], where the QoS problem is researched. We extended the approach therein for the MMF problem. In this paper, SDR-C solves the sub-problems $\mathcal{P}_1^{\text{hyb}}$, $\mathcal{P}_2^{\text{hyb}}$, $\mathcal{P}_3^{\text{hyb}}$ in alternate manner over $N_{\text{iter}}^{\text{SDR}} = 3$ iterations. The initialization of \mathbf{m} and $\{\mathbf{w}_k\}_{k=1}^K$ are the same as for LB-GDM (see line 1 of Algorithm 4). The SDR-C scheme is discussed in Appendix B.

Optimality: The proposed schemes, LB-GDM and SDR-C, cannot ensure global optimality. However, by observing Fig. 1 and Fig. 3 we corroborate that the approaches converge to a local optima for increasing N_{xpr} , N_{xpt} or N_{rand} .

Impact of number of constraints: It is well known that the optimality-gap of SDR degrades with increasing number of constraints (i.e., number of users K). As a result, we observe that for large K , the performance difference between LB-GDM and SDR-C increases, which indicates that LB-GDM is more robust and less sensitive to the number of constraints.

VII. CONCLUSION

In this paper, we investigated the design of fully-digital and hybrid precoders for single-group multicasting using a learning-based scheme. With the aim of maximizing the minimum SNR, our proposed low-complexity LB-GDM uses only matrix multiplications/additions and low-dimensional matrix inversion operations. We compare the performance of precoders based on SDR-C and LB-GDM under diverse simulation settings. The numerical results show a substantial gain, where LB-GDM outperforms SDR-C by up to 105.6% and 101.4% for digital and hybrid precoders, respectively. In addition, we demonstrate the importance of incorporating more receive antennas, where we achieve 75.7% and 100% gains in terms of the minimum SNR by increasing the number of receive antennas from one to two.

VIII. ACKNOWLEDGMENT

This research was in part funded by the Deutsche Forschungsgemeinschaft (DFG) within the B5G-Cell project as part of the SFB 1053 MAKI.

APPENDIX A GRADIENT OF J_k^F IN ALGORITHM 1

Let us define $\mathbf{u} = \mathbf{F}^H \mathbf{H}_k^H \mathbf{w}_k$ and $\mathbf{Y} = \mathbf{F}^H \mathbf{F}$. Then, the following differentials are computed: $d\mathbf{u} = d\mathbf{F}^H \mathbf{H}_k^H \mathbf{w}_k$, $d\mathbf{Y} = \mathbf{F}^H d\mathbf{F}$, $d\mathbf{u}^H = \mathbf{w}_k^H \mathbf{H}_k d\mathbf{F}$ and $d\mathbf{Y}^{-1} = -\mathbf{Y}^{-1} d\mathbf{Y} \mathbf{Y}^{-1}$. Thus, the differential of $J_k^F = \mathbf{u}^H \mathbf{Y}^{-1} \mathbf{u}$ is given by

$$\begin{aligned} dJ_k^F &= (d\mathbf{u}^H) \mathbf{Y}^{-1} \mathbf{u} + \mathbf{u}^H (d\mathbf{Y}^{-1}) \mathbf{u} + \mathbf{u}^H \mathbf{Y}^{-1} (d\mathbf{u}) \\ &= (\mathbf{w}_k^H \mathbf{H}_k d\mathbf{F}) \mathbf{Y}^{-1} \mathbf{u} - \mathbf{u}^H (\mathbf{Y}^{-1} d\mathbf{Y} \mathbf{Y}^{-1}) \mathbf{u} \\ &= (\mathbf{w}_k^H \mathbf{H}_k d\mathbf{F}) \mathbf{Y}^{-1} \mathbf{u} - \mathbf{u}^H (\mathbf{Y}^{-1} \mathbf{F}^H d\mathbf{F} \mathbf{Y}^{-1}) \mathbf{u} \\ &= \text{Tr} \left\{ \mathbf{Y}^{-1} \mathbf{u} \mathbf{w}_k^H \mathbf{H}_k d\mathbf{F} \right\} - \text{Tr} \left\{ \mathbf{Y}^{-1} \mathbf{u} \mathbf{u}^H \mathbf{Y}^{-1} \mathbf{F}^H d\mathbf{F} \right\} \\ &= \text{Tr} \left\{ \left(\mathbf{Y}^{-1} \mathbf{u} \mathbf{w}_k^H \mathbf{H}_k - \mathbf{Y}^{-1} \mathbf{u} \mathbf{u}^H \mathbf{Y}^{-1} \mathbf{F}^H \right) d\mathbf{F} \right\} \end{aligned}$$

The Frobenius inner product of two matrices \mathbf{P} and \mathbf{Q} is defined as $\mathbf{P} : \mathbf{Q} \equiv \text{Tr} \{ \mathbf{P}^T \mathbf{Q} \}$. Thus, $dJ_k^F = (\mathbf{Y}^{-1} \mathbf{u} \mathbf{w}_k^H \mathbf{H}_k - \mathbf{Y}^{-1} \mathbf{u} \mathbf{u}^H \mathbf{Y}^{-1} \mathbf{F}^H)^T : d\mathbf{F}$. Upon replacing \mathbf{u} in the expression above, we obtain

$$\nabla_{\mathbf{F}} J_k^F = (\mathbf{I} - \mathbf{F} \mathbf{F}^\dagger)^T (\mathbf{F}^\dagger \mathbf{H}_k^H \mathbf{w}_k \mathbf{w}_k^H \mathbf{H}_k)^T, \quad (\text{A.1})$$

where $\mathbf{F}^\dagger = (\mathbf{F}^H \mathbf{F})^{-1} \mathbf{F}^H$. Note that the Wirtinger derivative of J_k^F with respect to \mathbf{F}^* is zero, i.e., $\nabla_{\mathbf{F}^*} J_k^F = \nabla_{\mathbf{F}^H} J_k^F = \mathbf{0}$.

APPENDIX B SDR-C SCHEME

B.1. Optimization of \mathbf{F}

Assuming that $\{\mathbf{w}_k\}_{k=1}^K$ and \mathbf{m} are known, notice that we can express $\mathbf{F} \mathbf{m} = \mathbf{P} \mathbf{f}$, where $\mathbf{P} = \mathbf{m}^T \otimes \mathbf{I}$ and $\mathbf{f} = \text{vec}(\mathbf{F})$. Furthermore, if we assign $t = \min_{k \in \mathcal{K}} \frac{|\mathbf{w}_k^H \mathbf{H}_k \mathbf{F} \mathbf{m}|^2}{\sigma^2 P_{\text{tx}}^{\text{max}}}$, then $\mathcal{P}_1^{\text{hyb}}$ in (4) can be equivalently expressed as,

$$\mathcal{P}_1^{\text{hyb}} : \max_{\mathbf{F}} t \quad (\text{B.1a})$$

$$\text{s.t.} \quad \left| \mathbf{w}_k^H \mathbf{H}_k \mathbf{P} \mathbf{f} \right|^2 \geq t, \quad (\text{B.1b})$$

$$\|\mathbf{P} \mathbf{f}\|_2^2 = P_{\text{tx}}^{\text{max}}, \quad (\text{B.1c})$$

$$[\mathbf{f}]_n \in \mathcal{F}, n \in \mathcal{N}, \quad (\text{B.1d})$$

where $\mathcal{N} = \{1, 2, \dots, N_{\text{tx}} N_{\text{tx}}^{\text{RF}}\}$. In (B.1), realize that $\|\mathbf{P} \mathbf{f}\|_2^2 = \text{Tr}(\mathbf{X} \mathbf{D})$, with $\mathbf{X} = \mathbf{P}^H \mathbf{P}$ and $\mathbf{D} = \mathbf{f} \mathbf{f}^H$. Also, $[\mathbf{D}]_{n,n} = \delta_{\text{tx}}$ since $[\mathbf{f}]_n \in \mathcal{F}$. By noticing that $|\mathbf{w}_k^H \mathbf{H}_k \mathbf{P} \mathbf{f}|^2 = \text{Tr}(\mathbf{R}_k \mathbf{D})$, with $\mathbf{R}_k = \mathbf{P}^H \mathbf{H}_k^H \mathbf{w}_k \mathbf{w}_k^H \mathbf{H}_k \mathbf{P}$, (B.1) can be recast in its SDR form as shown in (B.2)

$$\mathcal{P}_{\text{SDR},1}^{\text{hyb}} : \max_{\mathbf{D}} t \quad (\text{B.2a})$$

$$\text{s.t.} \quad \text{Tr} \{ \mathbf{R}_k \mathbf{D} \} \geq t, \quad (\text{B.2b})$$

$$[\mathbf{D}]_{n,n} = \delta_{\text{tx}}, n \in \mathcal{N}, \quad (\text{B.2c})$$

$$\mathbf{D} \succcurlyeq \mathbf{0}, \quad (\text{B.2d})$$

where the constraint $\text{rank}(\mathbf{D}) = 1$ has been dropped. Also, (B.2d) enforces \mathbf{D} to be Hermitian positive semidefinite (PSD). Note that (B.2d) is linear in the PSD domain, and thus can be effectively approached by optimization solvers such as SDPT3. Upon obtaining \mathbf{D} , \mathbf{f} is recovered in three stages.

Stage 1: Observe that any element (n_1, n_2) of matrix \mathbf{D} can be represented as $[\mathbf{D}]_{n_1, n_2} = [\mathbf{f}]_{n_1} [\mathbf{f}]_{n_2}^*$. Now, let us define a vector $\mathbf{u} \in \mathbb{C}^{N_{\text{tx}}^{\text{RF}} \times 1}$ such that $\|\mathbf{u}\|_2^2 = \mathbf{u}^H \mathbf{u} = 1$. Thus, we can express $[\mathbf{D}]_{n_1, n_2}$ in terms of \mathbf{u} , i.e., $[\mathbf{D}]_{n_1, n_2} =$

$([\mathbf{f}]_{n_1} \mathbf{u}^T) ([\mathbf{f}]_{n_2}^* \mathbf{u}^*)$. Assuming that $\mathbf{q}_n = [\mathbf{f}]_n \mathbf{u}$, \mathbf{D} can be recast as $\mathbf{D} = \mathbf{Q}^T \mathbf{Q}^*$ with $\mathbf{Q} = [\mathbf{q}_1, \mathbf{q}_2, \dots, \mathbf{q}_{N_{\text{tx}} N_{\text{tx}}^{\text{RF}}}]$.

Stage 2: If the solution returned by $\mathcal{P}_{\text{SDR},1}^{\text{hyb}}$ is denoted by $\hat{\mathbf{D}}$. Then, via Cholesky decomposition we can obtain $\hat{\mathbf{D}} = \hat{\mathbf{Q}}^T \hat{\mathbf{Q}}^*$, where $\hat{\mathbf{Q}} = [\hat{\mathbf{q}}_1, \hat{\mathbf{q}}_2, \dots, \hat{\mathbf{q}}_{N_{\text{tx}} N_{\text{tx}}^{\text{RF}}}]$. In the previous stage, the premise was that each \mathbf{q}_n could be obtained from the same \mathbf{u} , since $\mathbf{q}_n = [\mathbf{f}]_n \mathbf{u}$. However, we cannot guarantee that every $\hat{\mathbf{q}}_n$ in $\hat{\mathbf{D}}$ has the same stem $\hat{\mathbf{u}}$. Although we have found $\hat{\mathbf{D}}$, \mathbf{f} and $\hat{\mathbf{u}}$ remain unknown.

Stage 3: The objective is to find some $\hat{\mathbf{u}}$ such that it originates the least error in the 2-norm sense, i.e.,

$$\mathcal{P}_{\text{LS},1}^{\text{hyb}} : \min_{\hat{\mathbf{u}}, [\mathbf{f}]_n, \forall n \in \mathcal{N}} \sum_{n=1}^{N_{\text{tx}} N_{\text{tx}}^{\text{RF}}} \|\hat{\mathbf{q}}_n - [\mathbf{f}]_n \hat{\mathbf{u}}\|_2^2 \quad (\text{B.3a})$$

$$\text{s.t.} \quad \|\hat{\mathbf{u}}\|_2^2 = 1, \quad (\text{B.3b})$$

$$[\mathbf{f}]_n \in \mathcal{F}, n \in \mathcal{N}. \quad (\text{B.3c})$$

Minimizing simultaneously over both $\hat{\mathbf{q}}_n$ and $\hat{\mathbf{u}}$ is challenging. If we assume that $\hat{\mathbf{u}}$ is known such that (8b) is satisfied, then we are required to solve

$$\tilde{\mathcal{P}}_{\text{LS},1}^{\text{hyb}} : \min_{[\mathbf{f}]_n, \forall n \in \mathcal{N}} \sum_{n=1}^{N_{\text{tx}} N_{\text{tx}}^{\text{RF}}} \|\hat{\mathbf{q}}_n - [\mathbf{f}]_n \hat{\mathbf{u}}\|_2^2 \quad (\text{B.4a})$$

$$\text{s.t.} \quad [\mathbf{f}]_n \in \mathcal{F}, n \in \mathcal{N}. \quad (\text{B.4b})$$

By expanding (B.4a), we realize that $\|\hat{\mathbf{q}}_n - [\mathbf{f}]_n \hat{\mathbf{u}}\|_2^2 = \hat{\mathbf{q}}_n^H \hat{\mathbf{q}}_n - 2\Re([\mathbf{f}]_n \hat{\mathbf{q}}_n^H \hat{\mathbf{u}}) + |[\mathbf{f}]_n|^2 \hat{\mathbf{u}}^H \hat{\mathbf{u}}$. Thus, (B.4) is

$$\tilde{\mathcal{P}}_{\text{LS},1}^{\text{hyb}} : \max_{[\mathbf{f}]_n, \forall n \in \mathcal{N}} \sum_{n=1}^{N_{\text{tx}} N_{\text{tx}}^{\text{RF}}} \Re([\mathbf{f}]_n \hat{\mathbf{q}}_n^H \hat{\mathbf{u}}) \quad (\text{B.5a})$$

$$\text{s.t.} \quad [\mathbf{f}]_n \in \mathcal{F}, n \in \mathcal{N}. \quad (\text{B.5b})$$

Note that (B.5) can be decomposed into $N_{\text{tx}} N_{\text{tx}}^{\text{RF}}$ independent sub-problems. Thus, since $z_n = \hat{\mathbf{q}}_n^H \hat{\mathbf{u}}$ is known, we need to select $[\mathbf{f}]_n$ such that the real part of (B.5a) is maximized. This is equivalent to choosing $[\mathbf{f}]_n$ with the closest phase to z_n^* . After finding \mathbf{f} , it can be reshaped to obtain \mathbf{F} .

B.2. Optimization of \mathbf{m}

We assume herein that \mathbf{F} and $\{\mathbf{w}_k\}_{k=1}^K$ are known. Thus, the SDR form of $\mathcal{P}_2^{\text{hyb}}$ is given by

$$\mathcal{P}_{\text{SDR},2}^{\text{hyb}} : \max_{t, \mathbf{M}} t \quad (\text{B.6a})$$

$$\text{s.t.} \quad \text{Tr}(\mathbf{Z}_k \mathbf{M}) \geq t, \quad (\text{B.6b})$$

$$\text{Tr}(\mathbf{Y} \mathbf{M}) = P_{\text{tx}}^{\text{max}}, \quad (\text{B.6c})$$

$$\mathbf{M} \succeq \mathbf{0}, \quad (\text{B.6d})$$

where $\mathbf{Y} = \mathbf{F}^H \mathbf{F}$, $\mathbf{Z}_k = \mathbf{F}^H \mathbf{H}_k^H \mathbf{w}_k \mathbf{w}_k^H \mathbf{H}_k \mathbf{F}$ and $\mathbf{M} = \mathbf{m} \mathbf{m}^H$.

B.3. Optimization of \mathbf{w}_k

Now, we assume that \mathbf{F} and \mathbf{m} are given. Therefore, SDR form of $\mathcal{P}_3^{\text{hyb}}$ is

$$\mathcal{P}_{\text{SDR},3}^{\text{hyb}} : \max_{t, \{\mathbf{W}_k\}_{k=1}^K} t \quad (\text{B.7a})$$

$$\text{s.t.} \quad \text{Tr}(\mathbf{C}_k \mathbf{W}_k) \geq t, \quad (\text{B.7b})$$

$$\text{Tr}(\mathbf{W}_k) = P_{\text{rx}}^{\text{max}}, \quad (\text{B.7c})$$

$$\mathbf{W}_k \succeq \mathbf{0}, k \in \mathcal{K}, \quad (\text{B.7d})$$

where $\mathbf{W}_k = \mathbf{w}_k \mathbf{w}_k^H$ and $\mathbf{C}_k = \mathbf{H}_k \mathbf{F} \mathbf{m} \mathbf{m}^H \mathbf{F}^H \mathbf{H}_k^H$. The problems $\mathcal{P}_{\text{SDR},1}^{\text{hyb}}$, $\mathcal{P}_{\text{SDR},2}^{\text{hyb}}$ and $\mathcal{P}_{\text{SDR},3}^{\text{hyb}}$ can be straightforwardly recast as linear programs and can therefore be efficiently solved by numerical solvers. In our case, we employed CVX and SDPT3.

REFERENCES

- [1] A. Biazon and M. Zorzi, "Multicast via Point to Multipoint Transmissions in Directional 5G mmWave Communications," *IEEE Communications Magazine*, vol. 57, no. 2, pp. 88–94, February 2019.
- [2] N. D. Sidiropoulos, T. N. Davidson, and Z. Luo, "Transmit Beamforming for Physical-Layer Multicasting," *IEEE Transactions on Signal Processing*, vol. 54, no. 6, pp. 2239–2251, June 2006.
- [3] L. Tran, M. F. Hanif, and M. Juntti, "A Conic Quadratic Programming Approach to Physical Layer Multicasting for Large-Scale Antenna Arrays," *IEEE Signal Processing Letters*, vol. 21, no. 1, pp. 114–117, January 2014.
- [4] B. Gopalakrishnan and N. D. Sidiropoulos, "High Performance Adaptive Algorithms for Single-Group Multicast Beamforming," *IEEE Transactions on Signal Processing*, vol. 63, no. 16, pp. 4373–4384, August 2015.
- [5] E. Karipidis, N. D. Sidiropoulos, and Z. Luo, "Quality of Service and Max-Min Fair Transmit Beamforming to Multiple Cochannel Multicast Groups," *IEEE Transactions on Signal Processing*, vol. 56, no. 3, pp. 1268–1279, March 2008.
- [6] E. Karipidis, N. D. Sidiropoulos, and Z. Q. Luo, "Transmit Beamforming of Multiple Co-Channel Multicast Groups," in *IEEE CAMSAP*, December 2005, pp. 109–112.
- [7] N. Bornhorst and M. Pesavento, "An Iterative Convex Approximation Approach for Transmit Beamforming in Multi-Group Multicasting," in *IEEE SPAWC*, June 2011, pp. 426–430.
- [8] A. Schad and M. Pesavento, "Max-min Fair Transmit Beamforming for Multi-Group Multicasting," in *WSA*, March 2012, pp. 115–118.
- [9] D. Christopoulos, S. Chatzinotas, and B. Ottersten, "Weighted Fair Multicast Multigroup Beamforming Under Per-antenna Power Constraints," *IEEE Transactions on Signal Processing*, vol. 62, no. 19, pp. 5132–5142, October 2014.
- [10] O. T. Demir and T. E. Tuncer, "Multi-Group Multicast Beamforming for Simultaneous Wireless Information and Power Transfer," in *Eusipco*, August 2015, pp. 1356–1360.
- [11] M. Sadeghi, E. Björnson, E. G. Larsson, C. Yuen, and T. L. Marzetta, "Max-Min Fair Transmit Precoding for Multi-Group Multicasting in Massive MIMO," *IEEE Transactions on Wireless Communications*, vol. 17, no. 2, pp. 1358–1373, February 2018.
- [12] T. Kim, J. Park, J. Seol, S. Joeng, J. Cho, and W. Roh, "Tens of Gbps Support with mmWave Beamforming Systems for Next Generation Communications," in *IEEE GLOBECOM*, December 2013, pp. 3685–3690.
- [13] M. Dai and B. Clerckx, "Hybrid Precoding for Physical Layer Multicasting," *IEEE Communications Letters*, vol. 20, no. 2, pp. 228–231, February 2016.
- [14] M. Sadeghi, L. Sanguinetti, and C. Yuen, "Hybrid Precoding for Multi-Group Physical Layer Multicasting," in *EW*, May 2018, pp. 1–6.
- [15] J. Huang, Z. Cheng, E. Chen, and M. Tao, "Low-Complexity Hybrid Analog/Digital Beamforming for Multicast Transmission in mmWave Systems," in *IEEE ICC*, May 2017, pp. 1–6.
- [16] O. T. Demir and T. E. Tuncer, "Antenna Selection and Hybrid Beamforming for Simultaneous Wireless Information and Power Transfer in Multi-Group Multicasting Systems," *IEEE Transactions on Wireless Communications*, vol. 15, no. 10, pp. 6948–6962, October 2016.
- [17] J. Palacios, D. Steinmetzer, A. Loch, M. Hollick, and J. Widmer, "Adaptive Codebook Optimization for Beam Training on Off-the-Shelf IEEE 802.11ad Devices," in *ACM MOBICOM*, October 2018, pp. 241–255.
- [18] W. K. Ma, P. C. Ching, and Z. Ding, "Semidefinite Relaxation Based Multiuser Detection for M-Ary PSK Multiuser Systems," *IEEE Transactions on Signal Processing*, vol. 52, no. 10, pp. 2862–2872, October 2004.
- [19] L. F. Abanto-Leon, M. Hollick, and G. H. Sim, "Hybrid Precoding for Multi-Group Multicasting in mmWave Systems," in *IEEE GLOBECOM*, December 2019.
- [20] P. J. Werbos, "Beyond Regression: New Tools for Prediction and Analysis in the Behavioral Sciences," *Ph.D. thesis, Harvard University*, 1974.